Tridimensional measurements of the Barrel absorbers (Module 0)

P. Puzo

Laboratoire de l'Accélérateur Linéaire,
IN2P3 and Université Paris-11, Orsay.

P. Schwemling

Laboratoire de Physique Nucléaire et Hautes Energies,
IN2P3 and Universités Paris-6 and Paris-7, Paris.

ATL-LARG-2001-004
12/01/2001

Abstract

In this note we describe the principle of the measurements done on the ATLAS absorbers that have been fabricated for the module 0 of the Liquid Argon Electromagnetic Barrel Calorimeter. We explain how the measurements are used to reconstruct the tridimensional geometry of each absorber. We show the results obtained for module 0. The same kind of measurements will be done for the series absorbers.

Contents

1 Introduction

It is essential for the electromagnetic calorimeter to have a response as uniform as possible. As all non-uniformities araising from the mechanics cannot be corrected on the hardware after the construction of the detector, it is crucial to reduce them as much as possible before the assembly itself. It may of course be possible to some extent to calibrate out residual non-uniformities, by selecting in the real data special events where there is at least one couple of electromagnetic cluster of well known invariant mass (i.e., for example, electrons coming from the decays $Z \to e^+e^-$, $\Upsilon \to e^+e^-$ or $J/\psi \to e^+e^-$). However, it is a safe practice to try to reduce the inhomogeneities already at the construction stage.

In this note, we will focus on the reduction and control of non-homogeneities coming from the actual structure of each absorber. In the case of lead plates, the effect of non-homogeneities can be reduced by using pairing techniques. However, this requires relatively large storage space and elaborated handling systems. For the absorbers, it is not possible to use pairing techniques, due to the large storage volume that would be needed and the amount of handling this would imply. Since we cannot rely on pairing techniques to ensure the uniformity of the absorber characteristics, we have to monitor as precisely as possible and react as soon as possible on the fabrication chain if some parameters appear to change suddenly or drift slowly from absorber to absorber. In fact, the actual tridimensional geometry of the absorbers is only of marginal importance; deviations from the theoretical shape given by the CAD files will only alter slightly global characteristics like for example the inner and outer radius of the calorimeter. However, if all absorbers deviate in the same way and by the same amount from the theoretical shape the uniformity of the calorimeter will still be conserved; what is the most important is the fact that all the absorbers are as similar as possible.

Section 2 deals with the absorber fabrication. The principles of the geometrical control are described in section 3, while section 4 deals with the measured quantity and their reproducibility. The absorber dimensions achieved for Module 0 are described in section 5.

2 Absorber fabrication

The manufacturing process of the absorbers, the tools and machines used to do so are described in detail in the Liquid Argon TDR [1], to which the reader is referred for further details. We recall here only the most important aspects of the whole process.

The absorbers are made of a sandwich of lead, glue-impregnated fiber-glass (often called *prepreg*) and stainless steel. At first the sandwich is stacked flat on a special table, working like a waffle-iron with two trays which can be rotated around a central axis, each of the tray having the ability to retain (by vacuum) a sheet of material deposited onto it while it is rotated. To prepare one sandwich, one needs two lead plates (one of 1.53 mm thickness, going from $\eta = 0$ to $\eta = 0.8$, and one of 1.13 mm thickness, going from $\eta = 0.8$ to $\eta = 1.4$), four prepreg foils of two different thicknesses to cover the lead plates and ensure a constant thickness of the resulting sandwich, and two stainless steel plates to protect each side of the sandwich and ensure its mechanical stiffness. Once the sandwich is finished, it is pushed into the jaws of the bending machine. The bending machine gives the unpolymerized sandwich the shape of the finished absorber, which is then put into the gluing press. In this tool, the glue impregnating the fiber-glass is heated and polymerizes, leading to the finished absorber. After cooling and cleaning, the finished absorber is mounted on the bar gluing stand, where the G10 bars are glued to the accordion.

3 Principle of the geometrical control

The technique that has been chosen is to use a tridimensional, automated coordinate measuring machine. During the early prototyping phase of the detector, some dedicated control systems were thought of, providing measurements of selected geometrical parameters. However, it was felt that such dedicated systems did not provide sufficient flexibility for a reliable control, since it was impossible or at least very difficult to measure geometrical quantities that would not have been foreseen to be measured from the start. Only a tridimensional measuring machine did provide enough flexibility to give the possibility to make measurements in an evolutive manner. Furthermore, this kind of apparatus is the only one to be able to measure the geometry of both faces of the absorbers and to measure the thickness of the absorber over its whole surface.

The tridimensional coordinate measuring machine, or CMM, is essentially a stable table of marble, plus three motorized axes equipped with precise position encoders and a contact-detecting measurement head. When the measurement head comes into contact with any material surface, the contact is detected, the

position of the encoders read out and stored by a data acquisition and control computer, before processing to reconstruct geometrical elements like planes, cylinders, holes, lines etc. This processing is directly done by the data acquisition computer, and the results stored on a file, that can be further analysed by the user. All the results that will be presented here have been deduced from these result files.

3.1 Calibration of the CMM

The calibration of the CMM is done according to a standard procedure, devised by the manufacturer of the machine. The basis of the calibration procedure is to measure a sphere whose radius is known with high precision using the mechanical sensor in all the orientations that will be used during later measurements. In this way, any non-uniformities in the mechanical behaviour of the sensor in any particular direction (deformations, variations of stiffness etc) can be calibrated out. The procedure is highly automated, so that the speed at which the sensor comes into contact with the calibration sphere is as reproducible as possible.

The calibration has usually to be done only once per day, or after a mechanical incident, for example hitting violently the sensor on the object being measured. It should be noted that the machine includes an automatic compensation for temperature effects; it is equipped with temperature sensors on all the axes to correct the raw encoder measurements.

3.2 Absorber handling and measuring frame

The difficulty of the handling is that the absorbers are handled in horizontal position before the measurements, and that they have to be brought into vertical position for the measurement, since the vertical position is the standard position for this operation. It is however possible to do measurements with absorbers in the horizontal position. This is not the default measurement setup. It does not allow simultaneous access to both faces of the absorbers and yields less information on the geometry. In particular, it is impossible to measure the thickness of an absorber in horizontal position.

The absorbers are brought into the measurement room on a flat table. Once in this room, the measurement and handling frame is put in horizontal position, being hold by four cables. The whole manipulation is done using a small dedicated electrical crane. Once the frame is above the absorber, it is slowly lowered onto the absorber, and claws are used to hold the absorber onto the frame. At the time the frame is a few centimeters above the absorber, two axes at each extremity engage into two pivots at the extremities of the absorber handling table, to allow the absorber and the frame, once solidarized, to rotate into vertical position. Once in vertical position, the absorber and the frame can be safely lifted from the handling table and positioned over the rail. They are then lowered and adjusted into iron vees, that define the position reference of the frame on the measurement rail. A sketch of the measurement room, of the handling tools and of the CMM is shown in figure 1.

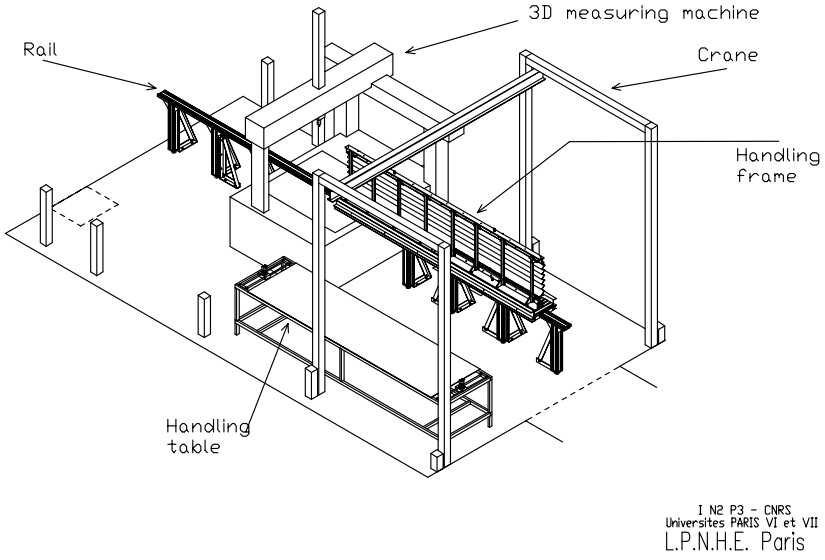

Figure 1: Sketch of the measurement room

Mechanically speaking, it should be noted that the absorbers have the outer bar rigidly fixed to the frame (through seven claws), while the inner bar is free. We have chosen this disposition because it is the closest possible to the situation where the absorber is completely free from any external force. In practice, the mounted absorber will be in a situation close to the completely locked case, i.e. where the bars have a rigidly fixed orientation in space, which should reduce the deformations with respect to the ones we are able to measure with our setup.

Since the absorbers are much longer than the marble table of the CMM, it is not possible to do all the measurements with the absorber in the same position. In practice, we have to do the measurement in three stages, the absorber being slid on the rail between each stage. This sliding is done manually, and the frame is positioned with a precision of the order of a millimeter with the help of an indexing pin.

4 Geometrical quantities measurement

4.1 Definition of the geometrical quantities measured

The following explanations are basic reminders about metrology. They explain how we have chosen our sensor radius and how the measuring machine translates raw positions into geometrical entities.

In principle, to reconstruct the geometry of an absorber, one could sense its shape with a sensor that should ideally be a sphere of zero radius, so that the positions given by the encoders on the three axes would give exactly the position of one point of the absorber. In practice, this is of course not possible, and one has to use a sensor with a finite radius. Furthermore, this radius has to be quite sizeable (a few millimeters), because of the rugosity of the surface of the absorber: a sensor with too small radius would be very sensitive to irregularities on the surface, but a too large one does not allow to probe small structures and would make the probing of the interiors of the folds of the absorber more difficult. In practice, we have found that a radius of 2.5 mm is a good compromise between the ease of use (the smaller the better) and the sensitivity to rugosity.

The largest difficulty to overcome with a sensor of a radius of a few millimeters is that in contrast to the idealized situation of a sensor reduced to a pin, the encoders do not give the position of a point of the surface of the absorber, but of the centre of a sphere that is tangent to the surface being measured, the plane tangent to the surface and to the sphere being of course unknown (see Fig 2). In practice, one has to determine this tangent plane in some way. This is usually done by specifying that the points to be measured do belong to a surface of known type (e.g. a sphere, a cylinder, a plane ...), whose exact equation has to be determined from the measurements. Mathematically speaking, once one knows the fonctional form of the equation of the surface to be measured, it is possible to deduce from this equation the equation of the surface on which the center of the sensor (i.e. the encoder positions) will be located. The equation of this sensor center surface contains a certain number of unknown parameters, that can easily be determined by a few measurements.

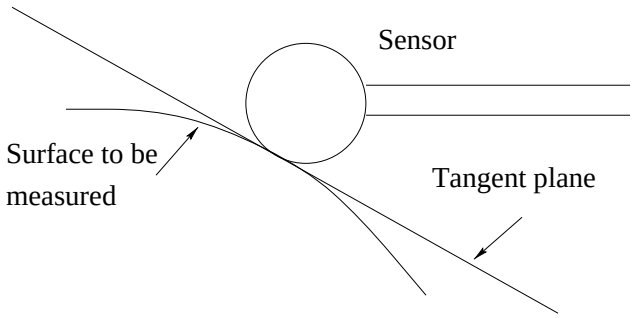

Figure 2: Sketch of the measurement of a surface

For example, if one wants to measure plane, then all the positions of the center will also be on a plane. This plane is of course parallel to the tangent plane for each measurement, and it can be reconstructed using a minimum of three measurements, this reconstruction being done by a least-squares method. Once this plane is known, one can determine the equation of the actual surface, knowing that it is parallel to the plane of the positions of the center of the sensor and at a distance which is the radius of the sensor.

For the purpose of our measurements, this means that we have to describe to the measuring machine the structure of the absorber in terms of geometrical objects, that have known equations. The basic objects we have chosen to use are *planes*, *segments* and *points*. From this we can deduce all the numerical values that we have used for our analyses :

- The *angles* are simply obtained by computing the angle between two planes belonging to the same fold.
- The *straight sections* are defined as the segment between two consecutive intersection points (see Fig 8 and 9), where each intersection is the point common to a plane perpendicular to the support frame and to the line intersection of two adjacent planes of the absorber.
- The *thicknesses* are defined as being the distance between one arbitrary point taken on one face of the absorber to the plane on the opposite side. This definition may be surprising; one must however remember that two real planes like the absorber surfaces are never mathematically parallel, so that their distance, mathematically speaking, is not defined, since they always intersect !

4.2 Reproducibility and resolution of the measurements

The reproducibility of the measurements has been studied for the measurement of angles and of distances, which are the basic quantities we are working with. This has been done on a given absorber which has been put on the measurement frame, and measured nine times. Between each measurement, the measurement frame has been removed from the rail, and put again in place before the next measurement. The results are shown Fig 3 for the straight sections, and Fig 4 for the angles (see Fig 8 and Fig 24 for the definitions of the straight section and angle numbers). As can be seen, the reproducibility of the straight sections, whose length is always about 60 mm, is of the order of a few microns. For the angles, the reproducibility is of the order of 0.004 degree for all the angles that it is possible to define between two consecutive straight sections.

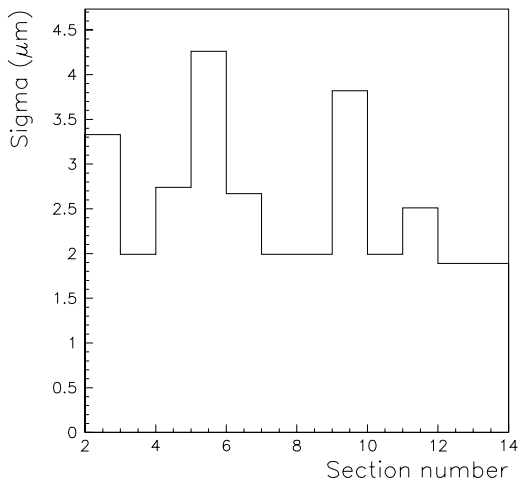

Figure 3: Reproducibility of the straight section length measurements, as a function of the section length number on the absorber. This reproducibility is evaluated as the r.m.s. of 9 measurements on one absorber. The length of each straight section is of the order of 50 to 60 mm

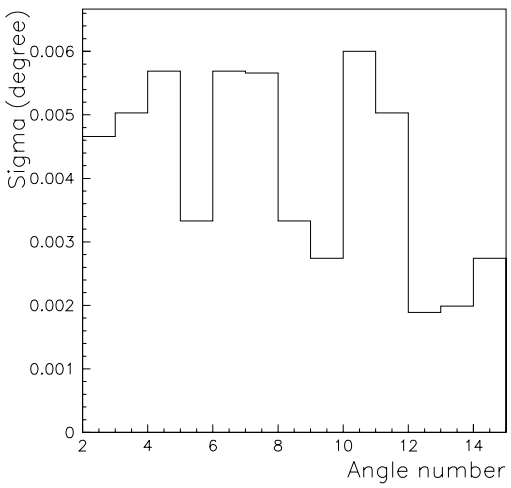

Figure 4: Reproducibility of the angle measurements, as a function of the angle number on the absorber. This reproducibility is evaluated as the r.m.s. of 9 measurements on one absorber

For the full width of the absorber, and for one of the half-widths, we have found that the reproducibility is of the order of 10 to 15 μm. This is in agreement with the technical specifications of the measuring machine, that state that the measurement accuracy tends to worsen linearly as the length measured increases.

To summarize, we have found that for the straight sections, the reproducibility of the measurements is a few microns, and about 15 μm for the longest lengths we are going to measure, i.e. the width of the absorber.

One of the most delicate points we wanted to check is the ability of the CMM to measure accurately the thickness of the absorbers. This is a difficult point for this machine, because to measure the thickness of the

absorbers, the measuring head has to travel over large distances (from one side of the absorber to the other side, passing over it, in the few centimeter space free above the handling frame and below the machine axes) and to rotate by 180°. Such long and complicated movements may degrade the precision of the positionning of the measuring head, with consequently lower precision results. For several absorbers, we have measured the thickness of the extremities of the absorber, at $z = 0$ and at $z = 3200$ mm, using a palmer, and we have compared these measurements with the thickness given by the CMM. The results of this comparison are shown figure 5. It appears that the correlation is very good, the difference between the results of the CMM and the palmer being distributed as a gaussian with a r.m.s. of about 10 microns, which is typically the accuracy one would expect for a manual measurement of the thickness. Attributing all of this r.m.s. to the CMM accuracy (which is certainly conservative), we can consider that the accuracy of the thickness measurement is of the order of 10 microns.

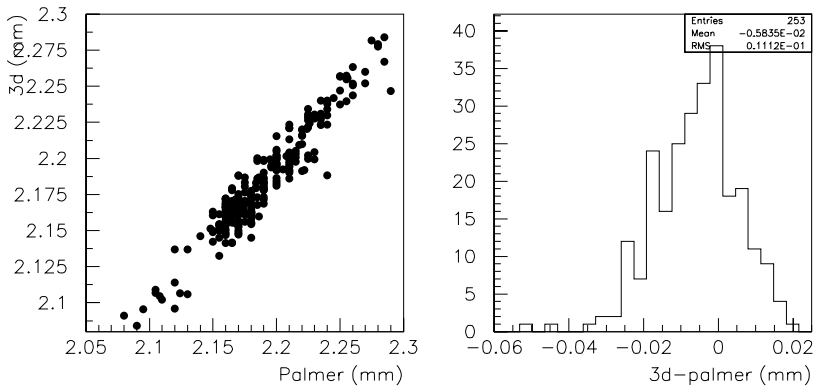

Figure 5: Study of the palmer vs CMM thickness measurements. Left : Correlation of both measurements. Right : Distribution of the measurement differences

We have also checked the measurements over quite long distances, by comparing the distance between bars measured with the CMM and with a very long palmer. The distribution of the difference of these measurements is shown figure 6. Although the mean is slightly shifted, the shift is compatible with the typical accuracy (0.1 mm) one expects from such measurements done by hand.

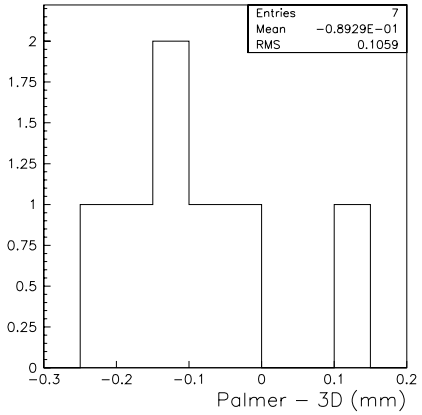

Figure 6: Distribution of the differences of distance between G10 bars, using palmer and CMM

5 Results on Module 0 absorbers

In this section we summarize the output of the measurements done on the Module 0 absorbers. The global shape will be studied in section 5.6. All 64 absorbers were measured vertically at seven locations in z (see Fig 7) along the absorber length (z =400, 800, 1200, 1600, 2000, 2400 and 2800 mm). As explained in section 3.2, the absorbers are moved three times during a complete measurement, leading to four different zones that are not connected together ({400, 800}, {1200}, {1600, 2000} and {2400, 2800}). This implies that we can not measure the absorber along its 3200 mm using the same reference frame for the machine, but only on smaller distances. In practice, this is not a limitation, since we do not need to "connect" points measured within one reference frame to points measured within another one, to measure quantities like straight section lengths, angles, thicknesses etc.

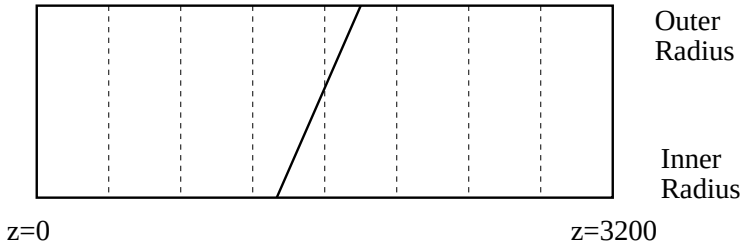

Figure 7: Schematics of the absorber with its two lead thicknesses and its seven measurement lines along z

Only few absorbers were also measured horizontally, since this position does not allow to measure the thickness. The following results are mainly deduced from the vertical measurements. Due to practical reasons for the assembling of the modules, the absorbers are labelled from 63 to 0. Fabrication of Module 0 absorbers started in January 1998 by absorber #63 and ended in July 1998 by absorber #0.

5.1 Length of straight sections

The 14 different straight sections of the absorbers (see Fig 8 and 9) were measured by the CMM as described in section 4.1.

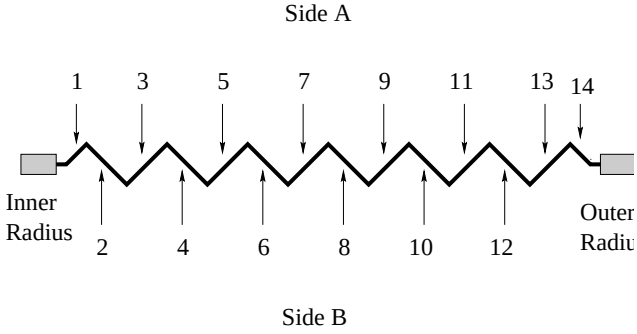

Figure 8: Schematics of an absorber with its 14 measured straight sections

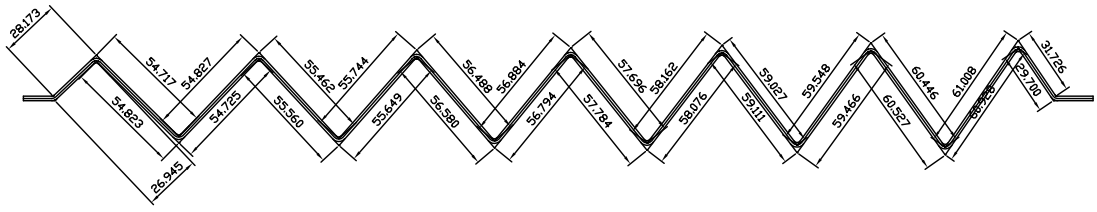

Figure 9: Theoretical values (in millimeters) of the straight section lengths, as taken from the official drawing at 20 °C (ATLABEA_001)

The deviations from theoretical value of the straight section lengths averaged over the 64 absorbers of Module 0, are given in Table 1 for all the measurement lines along the absorber length.

Straight Section z(mm)	1	2	3	4	5	6	7	8	9	10	11	12	13	14
400	.19	.02	.04	.04	.05	.08	.04	.05	.04	.04	.04	.02	.01	.16
800	.23	.02	.05	.05	.05	.09	.06	.06	.06	.06	.07	.04	.06	.23
1200	.19	.01	.05	.05	.05	.08	.06	.06	.06	.06	.09	.07	.07	.22
1600	.24	.01	.05	.05	.06	.08	.06	.06	.08	.08	.10	.07	.03	.21
2000	.24	.01	.05	.05	.06	.07	.06	.06	.07	.07	.10	.07	.04	.23
2400	.18	.02	.05	.05	.06	.06	.05	.05	.05	.05	.09	.06	.04	.19
2800	.14	.07	.06	.06	.08	.09	.06	.05	.06	.06	.08	.05	.07	.13

Table 1: Deviation from theoretical value of the average straight section lengths (in millimeters) for the 64 absorbers of Module 0, using vertical measurements done from side A of the absorbers

The stability of the measurement among the 64 absorbers is quite good (typically 3 10^{-4}). Figure 10 shows the distribution of the rms of all the measurements given in Table 1 for the inner sections (#2 to 13). Each entry is the rms among the 64 absorbers of a measurement at a given location in z and on a given straight section. The reproducibility of the absorber measurements is about 15 μm, as compared to the CMM reproducibility (2-3 μm, see 4.2). So there is definite evidence for absorber to absorber variations on the straight section length along the production of the module 0 absorbers. Indeed, on figure 12, it is obvious that the straight section lengths have drifted by typically 40-50 microns over the whole module 0 absorber production. However, it should be noted that during most of this production, the bending press parameters have been progressively tuned, which may explain the observed drifts.

The reproducibility on sections 1 and 14 is the worst (60 μm). This is clearly linked to a particularly large drift over time for these two sections. However, it should be noted that the these two sections are the least constrained by the bending press and the gluing press, and so are naturally the most prone to have strong variations.

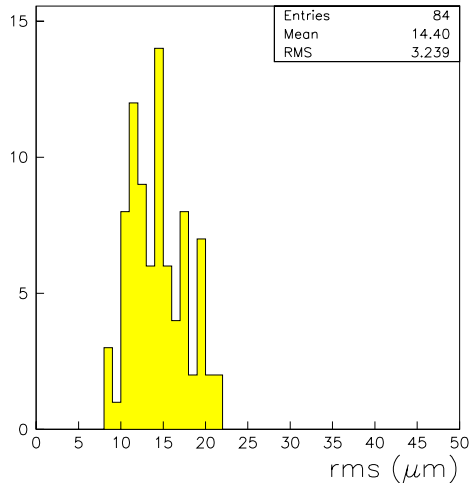

Figure 10: Distribution of the rms of all the measurements for the inner straight sections (#2 to 13), using vertical measurements done from side A of the absorbers. Each entry is an rms among the 64 absorbers of Module 0 of a variable whoose average value is given in Table 1

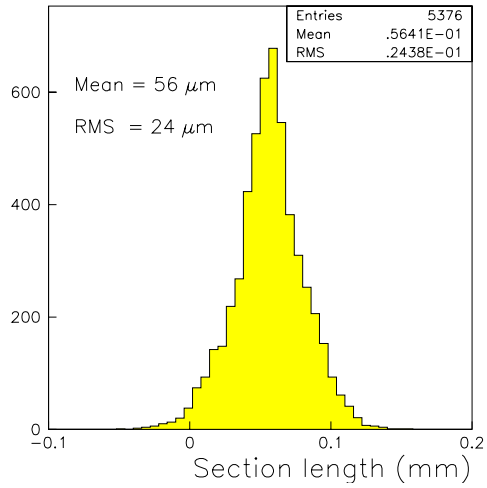

Figure 11: Distribution of the straight section lengths for all measurements in z and all inner sections (#2 to 13), using vertical measurements done from side A of the absorbers. The theoretical value is substracted for each entry

The distribution of all the straight section measurements is given in Fig 11. All lengths are on average 60 μm too long with respect to their theoretical value. The dispersion on that measurement (24 μm) is

significantly larger than the one on individual measurements (15 μm, see Fig 10). This implies a variation of the straight section dimension along the absorber length or along the absorber radius.

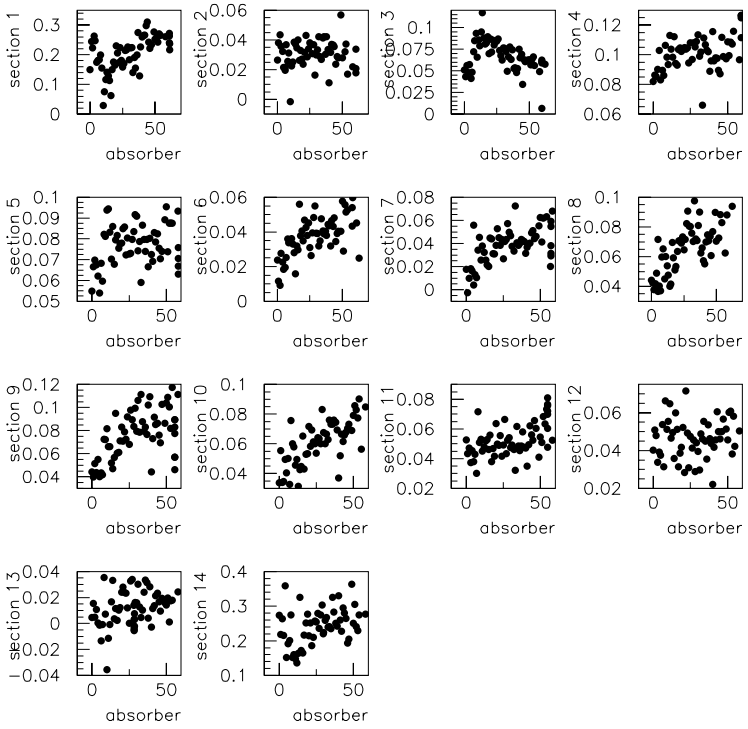

Figure 12: Deviatiom from theoretical value of straight section length as a function of absorber number, for all absorbers of the module 0, measured in section z=1200

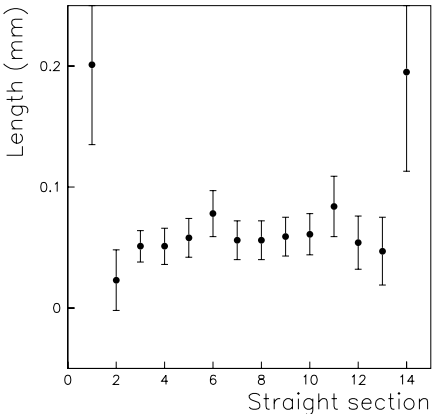

Figure 13: Deviatiom from theoretical value of the straight section length, averaged over z, using vertical measurements done from side A of the absorbers. The theoretical value is substracted for each entry

Figure 13 represents the length of the straight sections along the absorber radius, averaged over the absorber length. Not taking into account the extreme straight sections, all lengths are between 0.02 and 0.07 mm too long with respect to theoretical values, apart from sections 6 and 11 that are 0.08 mm too long. In any case, the straight section length are within 0.1 mm from their theoretical value.

The variation along the absorber length is displayed in Fig 14. One can distinguish 2 sets of straight sections: in the front sections #2 to 10, the mean length is rather constant along the absorber length, except for z=2800 for section 2, where it is higher by 0.1 mm. On the other side, in the rear sections #11 to 13, a structure is observed along the absorber length: the lengths are smaller in the middle of the absorber than on its sides. The size of the bump in the middle of section 11 reaches 50 μm.

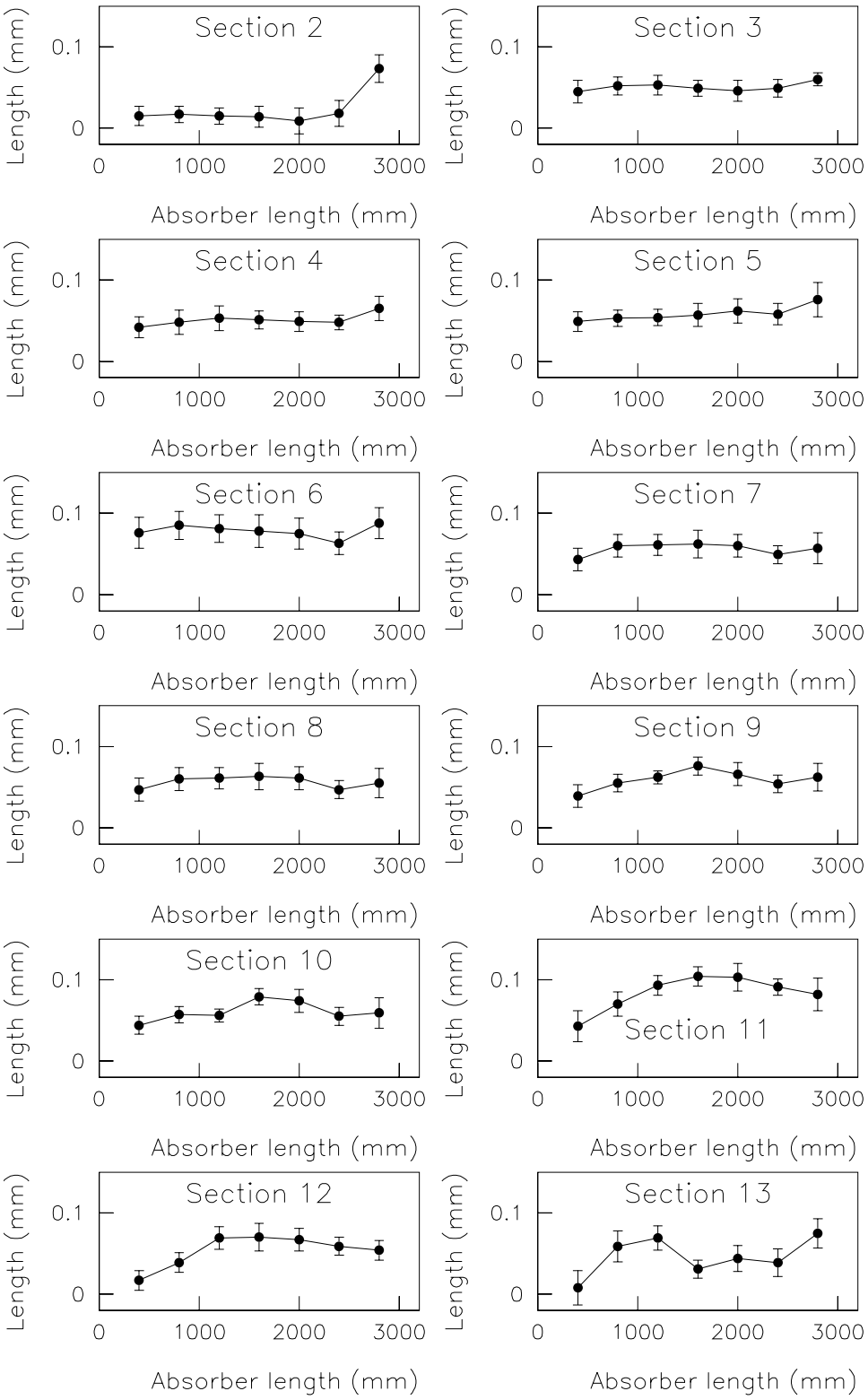

Figure 14: Variation of the straight section length for all the inner sections (#2 to 13) as function of the absorber length, using vertical measurements done from side A of the absorbers. The theoretical value is substracted for each entry

5.2 Overall absorber dimensions

Distances between extreme folds (see Fig 15) are used to monitor the quality of the production. They show (see Fig 16) that the distance between folds on the outer radius is varying by 0.3 mm along z, while the effect is much smaller for the most inner folds. This leads to the fact the absorbers are a little shrinked in the middle with respect to their extremities. One can notice that the deviation of the full width from its theoretical value is equal to the sum of the deviations of the half-widths from their respective theoretical values.

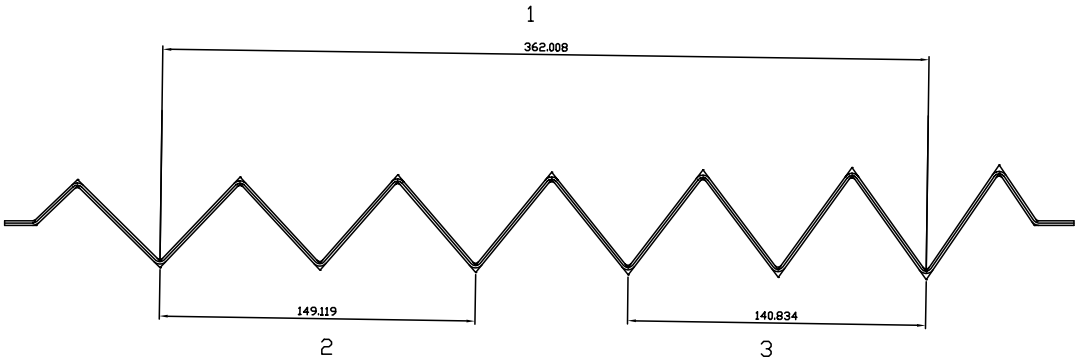

Figure 15: Theoretical values (in millimeters) of the overall absorber dimensions, as taken from the official drawing at 20 °C (ATLABEA_001)

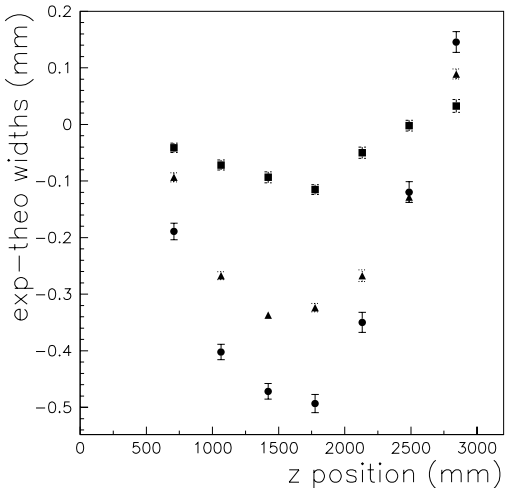

Figure 16: Deviation from theoretical value of widths between folds along the absorber length, using vertical measurements done from side A of the absorbers. Circles : width 1 on figure 15, i.e. full absorber length, squares : inner half-width of the absorber (width 2), triangles : outer half-width of the absorber (width 3)

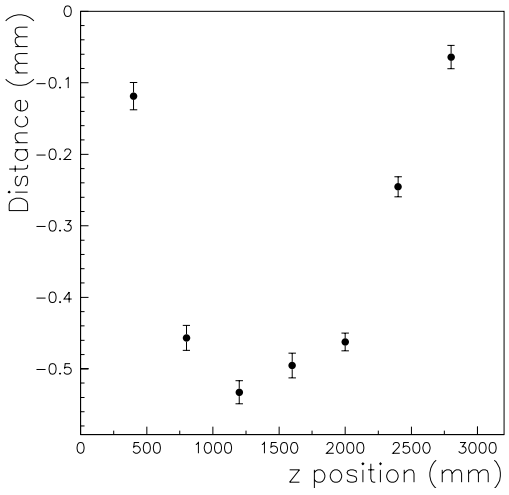

Figure 17: Variation of the distance between G10 bars as function of z, using vertical measurements done from side A of the absorbers. The theoretical value is subtracted for each entry.

The reproducibility of each of these measurements among the 64 absorbers is about 150 μm, while the reproducibility of the CMM itself on that type of measurement is of the same order of magnitude (see 4.2). We have investigated wether there were slow drifts over time, i.e. as a function of absorber number. This is represented in figures 18 to 21. It can be seen that the global absorber dimensions are quite stable, except towards the $z = 3200$ measurement line, where some drifts show up.

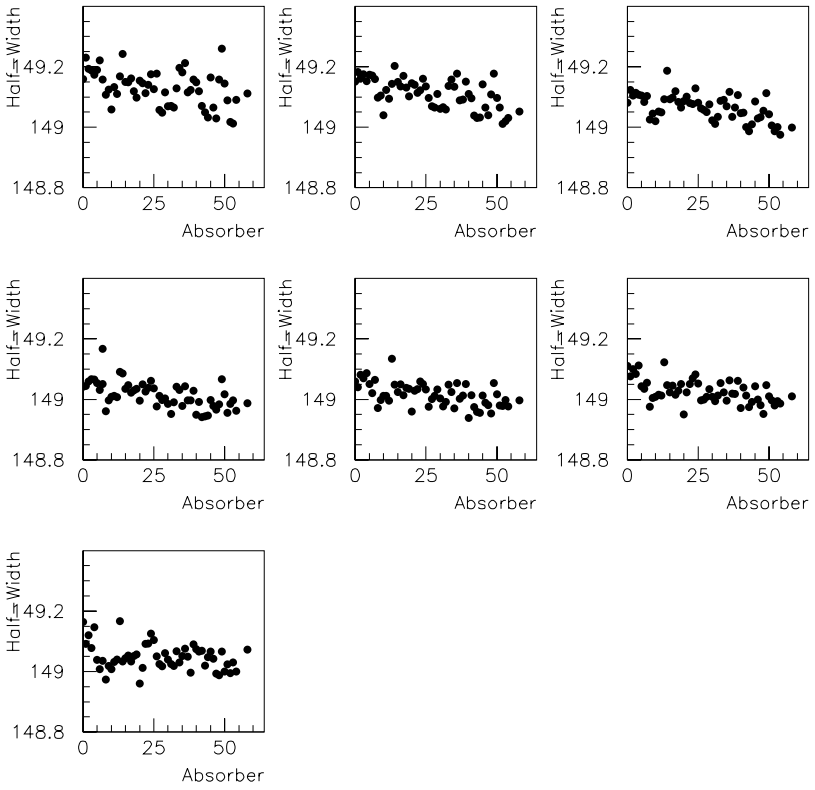

Figure 18: Inner Half-width as a function of absorber number, from $z = 400$ to $z = 2800$

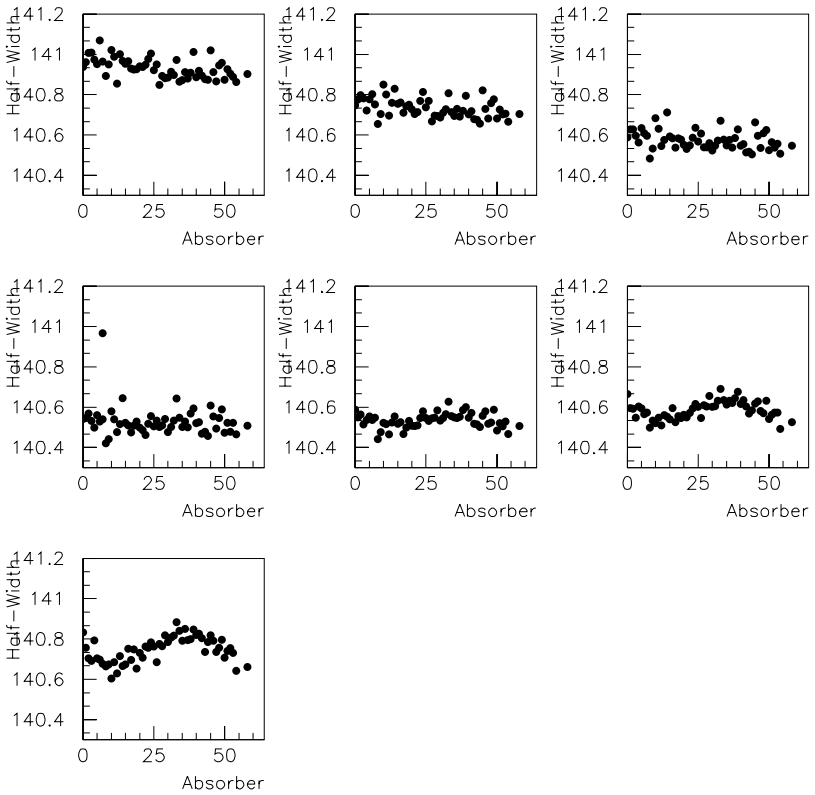

Figure 19: Outer Half-width as a function of absorber number, from $z = 400$ to $z = 2800$

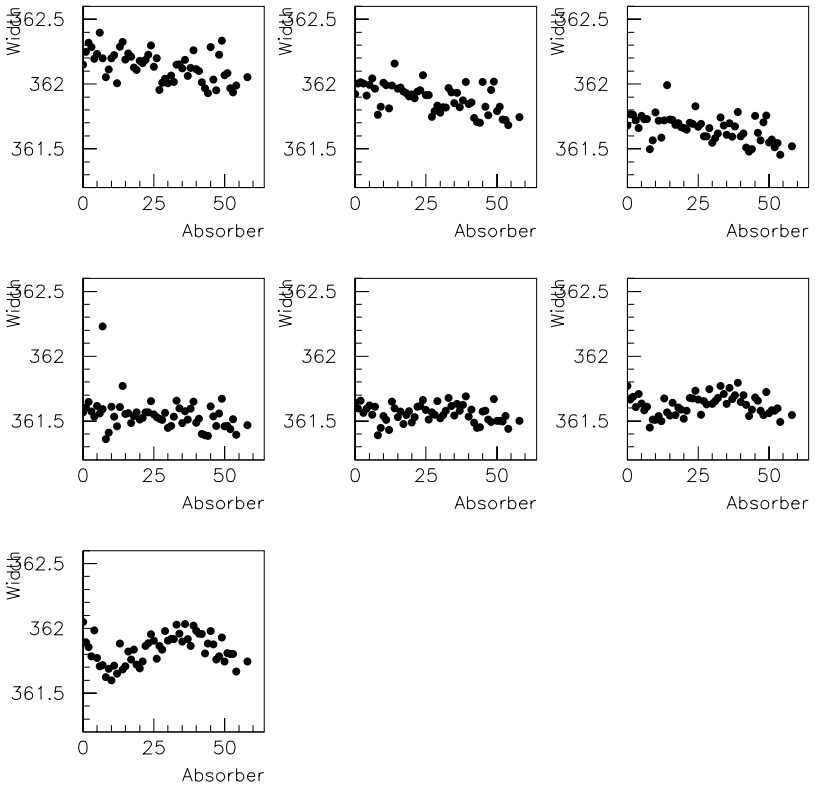

Figure 20: Absorber total width as a function of absorber number, from $z = 400$ to $z = 2800$

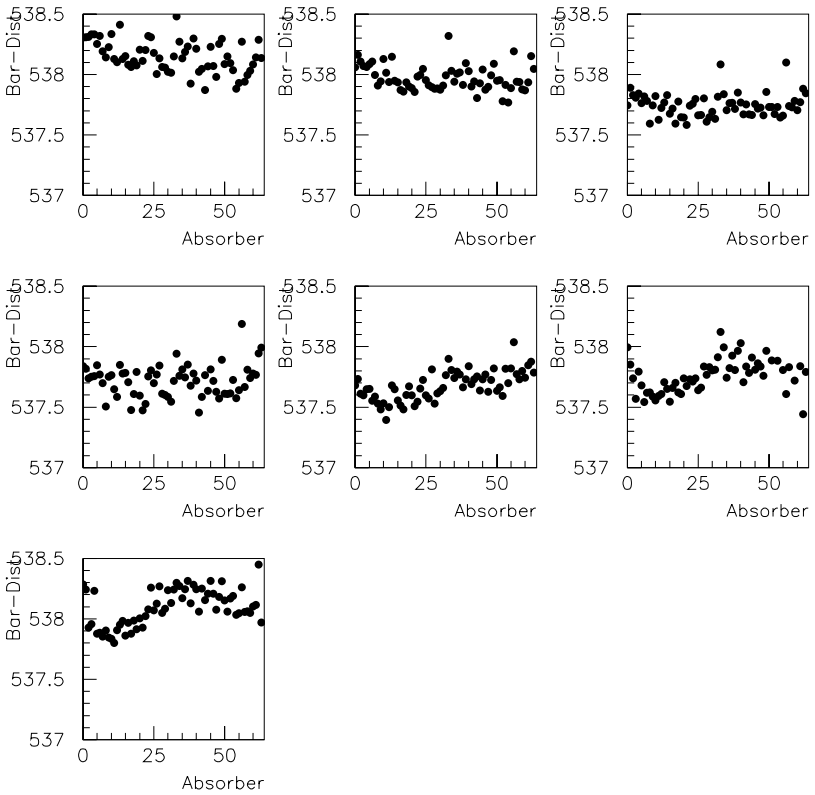

Figure 21: Bar to bar distance as a function of absorber number, from $z = 400$ to $z = 2800$

We have also investigated to which extent the total width of the absorbers and the distance between bars are correlated. When the bars are glued on the absorber, the absorber can be constrained by the gluing stand, and one expects this to reduce the propagation of the absorber width variation to the distance between bars. Figure 22 shows that indeed, the variations are somewhat reduced.

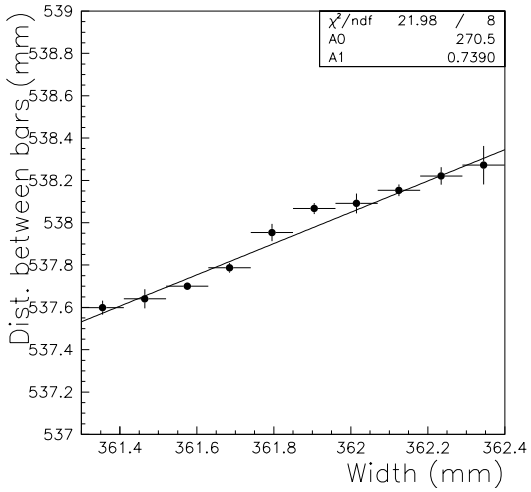

Figure 22: Correlation between bar to bar distance and absorber full width

5.2.1 Comparison between horizontal and vertical measurements

Some of the absorbers were measured in horizontal position, so we could compare how the absorber deforms its shape when going from horizontal to vertical position. Figure 23 shows, as a function of the position in z along the absorber, the difference between horizontal and vertical position for the total width and for the half-widths (see figure 15 for the definition of the widths and half-widths). Globally, one can see that the absorber tends to widen by about 0.1-0.2 mm when it is put vertically, but only at its extremities, the center part staying close to the dimensions of the horizontal absorber, with even some tendancy to shrink. We have checked that the sum of the differences for the two half-widths is line by line equals to the difference for the total width. Since the absorber in the detector will be blocked by the G10 bars at its extremities, this effect will in practice be greatly reduced.

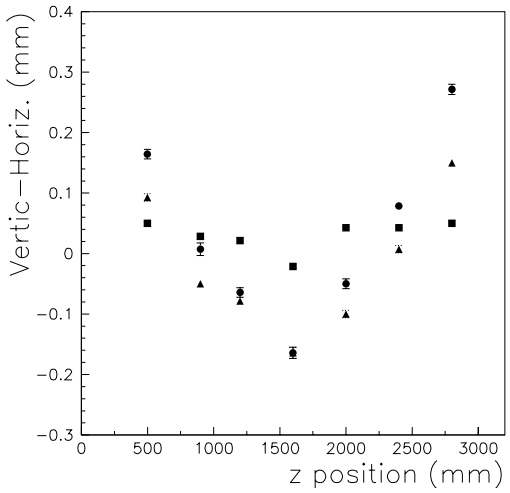

Figure 23: Comparison between global dimensions measured in horizontal and vertical position, as a function of the z position of the measurement on the absorber. Round dots are for the dimension labelled 1 on figure 15, i.e. for the full width, squares are for the dimension labelled 2, i.e. for the inner half-width, triangles for the dimension labelled 3, i.e. for the outer half-width

5.3 Angles

The 15 different angles of the accordeon structure (see Fig 24 and 25) were measured by the CMM as described in section 4.1.

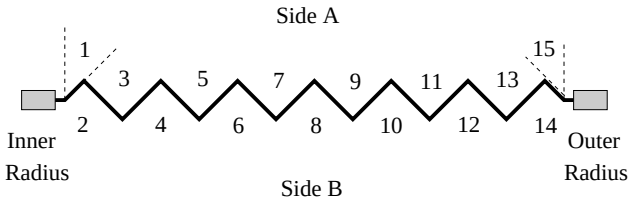

Figure 24: Schematics of an absorber with its 15 measured angles

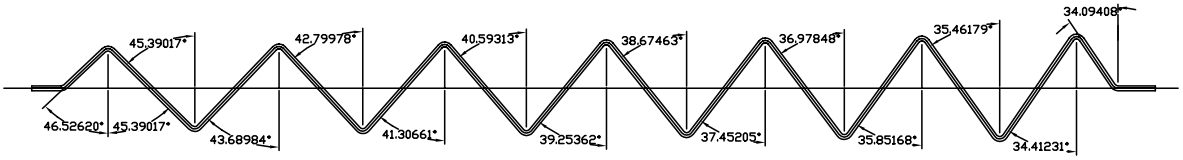

Figure 25: Theoretical values (in degrees) of the absorber angles, as taken from the official drawing at 20 °C (ATLABEA_001)

The deviations from theoretical value of the measured angles averaged over the 64 absorbers of Module 0, are given in Table 2.

Angle	1	2	3	4	5	6	7	8	9	10	11	12	13	14	15
z(mm)															
400	-.40	.03	-.15	-.04	-.14	-.14	-.19	-.04	-.14	-.01	-.09	.02	.06	.13	-.62
800	-1.87	.00	-.14	-.06	-.17	-.17	-.24	-.11	-.22	-.11	-.16	-.17	.01	-.19	-.77
1200	-.28	-.05	-.10	-.11	-.20	-.19	-.25	-.15	-.26	-.17	-.17	-.34	-.03	-.22	-.61
1600	-.59	-.07	-.07	-.13	-.22	-.23	-.25	-.17	-.28	-.24	-.28	-.37	-.06	.01	-.54
2000	-.46	-.07	-.07	-.12	-.22	-.24	-.25	-.16	-.25	-.21	-.23	-.36	-.05	-.24	-.52
2400	-.47	-.09	-.08	-.13	-.20	-.20	-.22	-.13	-.19	-.18	-.15	-.30	-.03	-.11	-.60
2800	-.61	-.29	-.16	-.14	-.21	-.22	-.20	-.11	-.10	-.14	-.08	-.15	-.04	-.14	-.68

Table 2: Deviation from theoretical value of mean angle (in degree) for the 64 absorbers of Module 0, using vertical measurements done from side A of the absorbers

The stability of the measurement among the 64 absorbers is typically 10^{-3}. Figure 27 represents the distribution of the rms of all the measurements for the inner angles (#3 to 13). Each entry is the rms among the 64 absorbers of a measurement at a given location in z. The reproducibility is below 8/100 degree, as compared to the CMM reproducibility (about 5/1000 degree, see figure 4). This leads to absorber to absorber variations of the angles along the production of the 64 absorbers. This is displayed in Fig 26 where one can see some drifts in the angle values, as a function of time.

For angles 2 and 14, the reproducibility is 15/100 degree, and 50/100 degree for angles 1 and 15. The reasons for the outer angles being less reproducible are the same that lead to the outer straight sections being less reproducible than the inner ones: the inox/prepreg/lead sandwich is the least constrained by the knives of the bending press at this position.

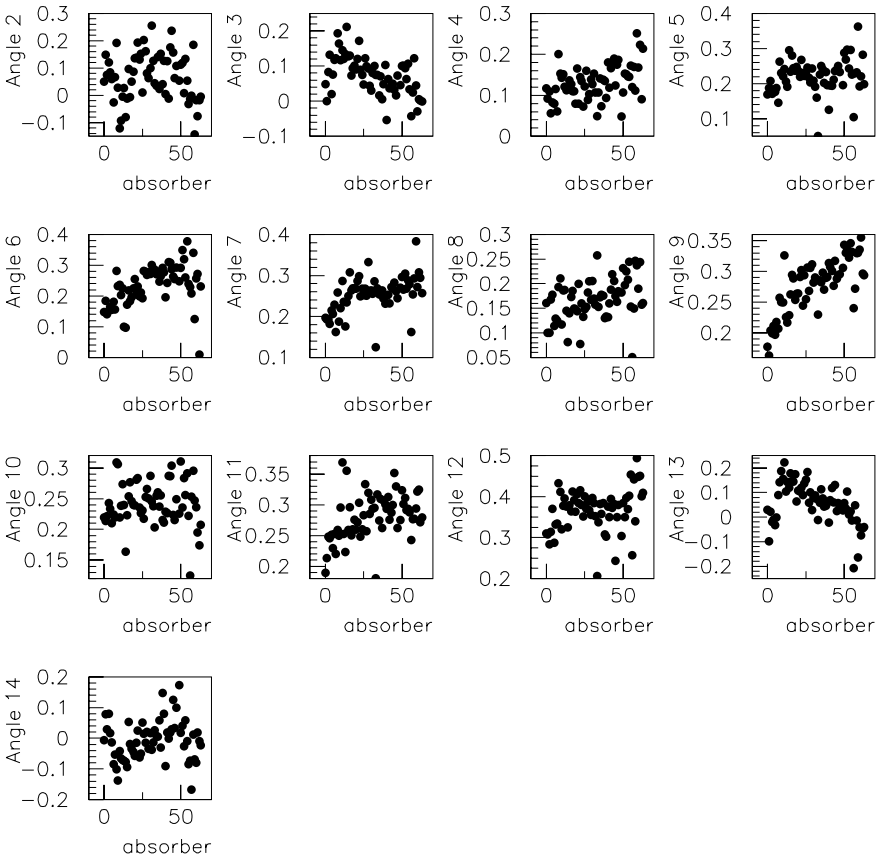

Figure 26: Angle values as a function of absorber number. The theoretical value is subtracted for each entry

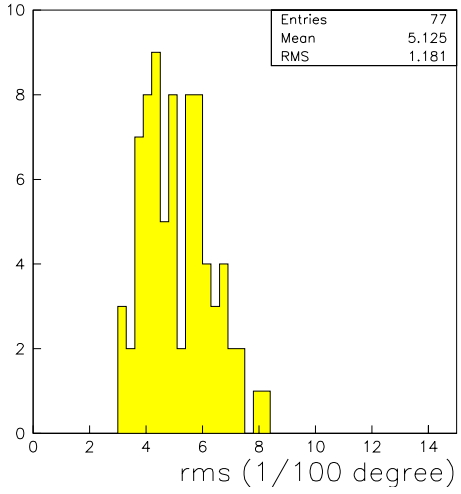

Figure 27: Distribution of the rms of all the measurements for the inner angles (#3 to 13), using vertical measurements done from the side A of the absorbers. Each entry is an rms among the 64 absorbers of Module 0

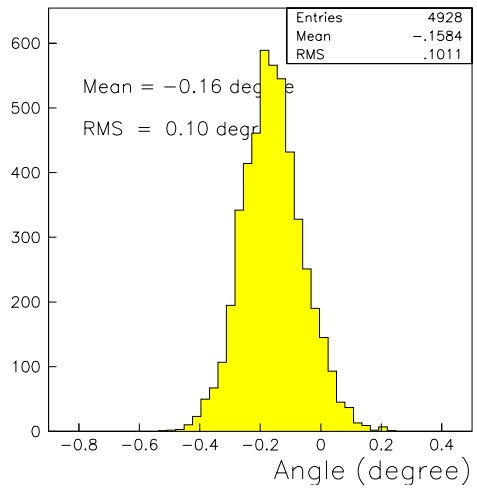

Figure 28: Distribution of the angles, for all measurements in z and all inner angles, using vertical measurements done from the side A of the absorbers. The theoretical value is substracted for each entry

The distribution of all the angle measurements is given in Fig 28. All angles are on average 0.16° too close with respect to their theoretical value. The dispersion on that measurement (0.1°) is twice as large as the one on individual measurements (see Fig 27). This imply a variation of the angles along the absorber length or along the absorber radius.

Figure 29 and 30 give the variation of the opening angle for all the absorber folds. Several types of angles can be observed: the front angles #3 to 7 are rather monitonic along the absorber length, while the rear angles #8 to 12 exhibit a strong dependance of the measurement on the longitudinal position which becomes larger for the outer angles. It goes to 3/10 degree for angle 12. Angles 1 and 15 are different from all the others. This is still due to the fact that the bend of the extreme part of the absorber, going towards the G10 bar, is not well controlled, neither in the bending machine nor in the gluing one.

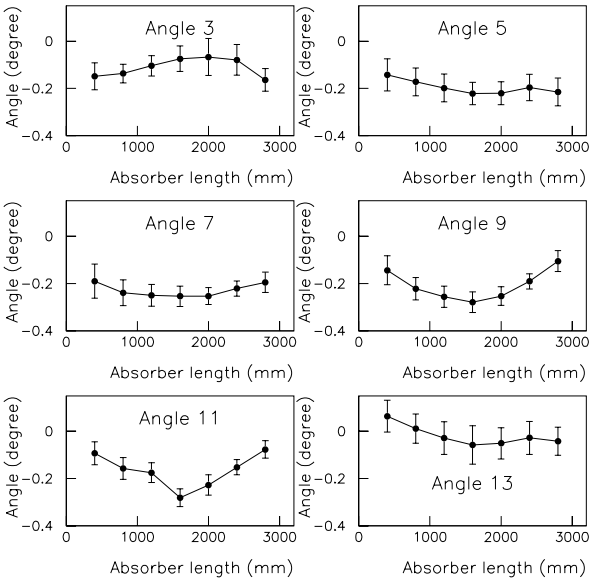

Figure 29: Variation of the angles along the absorber length, for the angles open on side A. Data are taken from vertical measurements done from side A of the absorbers. The theoretical value is substracted for each entry

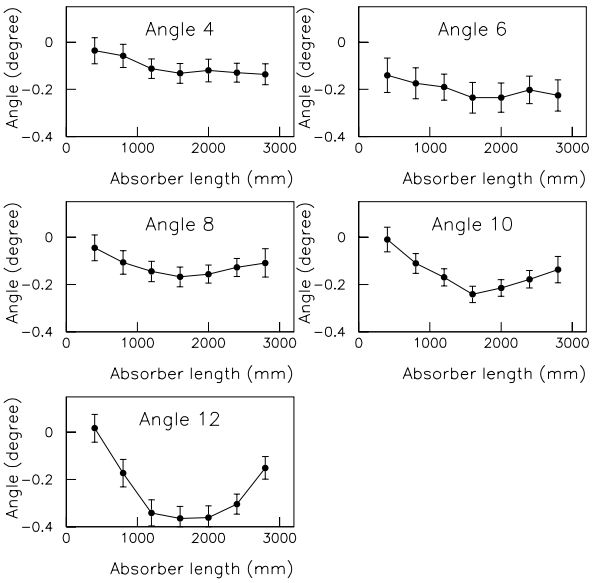

Figure 30: Variation of the angles along the absorber length, for the angles open on side B. Data are taken from vertical measurements done from side A of the absorbers. The theoretical value is substracted for each entry

Figure 31 represents the angles, averaged over z. All angles are 0.1 to 0.2 degree too close with respect to theoretical values. This is related to the fact that the absorber radius is too short: the straight sections are all slightly too long (by typically 60 μm), the angles are all slightly too closed (by typically 0.1 to 0.2 degree), but the net effect is that the overall absorber width is reduced (see section 5.2). The order of magnitude of both effects can be roughly evaluated as being :

- Total length increase of the straight sections :

$$\delta l = 0.06 \times \sin 40^\circ \times 13 = +0.5\ mm$$

  where 0.06 mm is the length increase of each straight section, 40° is the typical angle between each straight section and the absorber plane, and 13 is the equivalent number of straigh sections.

- Total length increase due to the angles closing

$$57 \times \frac{-0.2 \times \pi}{180} \times 13 \times \frac{\sin 40^\circ}{2} = -0.8\ mm$$

  where 57 is the typical length of each straight section, 0.2 is the typical angle reduction, 40° is the typical opening angle of each vee. The division by 2 accounts for the fact that each straight section is part of two angles.

The sum of both effects amounts to a shortening of about 0.3 mm, which is indeed the order of magnitude of the overall shortening found in section 5.2

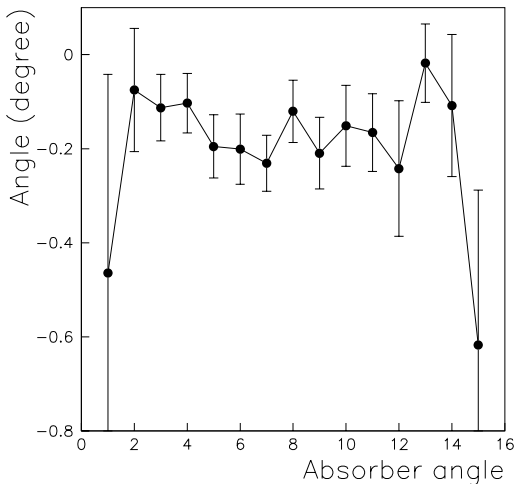

Figure 31: Variation of the angles, averaged over the absorber length, using vertical measurements done from side A of the absorbers. The theoretical value is substracted for each entry

5.3.1 Measurement from both sides of the absorber

We have compared the angles measured from both sides of the absorber, which makes sense because they can be defined theoretically on both sides of the absorber and should have the same value as measured from face A or B. The average difference between angles measured on face A and angles measured on face B, as a function of z position is plotted figure 32. One can see that (not very surprisingly !) the angles measured from both faces of the absorber are very close to each other, except for angle 14, where there is a clear dependance of the difference between the angles measured on both sides as a function of z. Furthermore, the fact that the difference is not consistent with zero indicates that one of the flanks used to construct this angle has a varying thickness along its length, this effect tending to increase towards high z. One has to note however that this thickness is not measured by the CMM (see section 4.1).

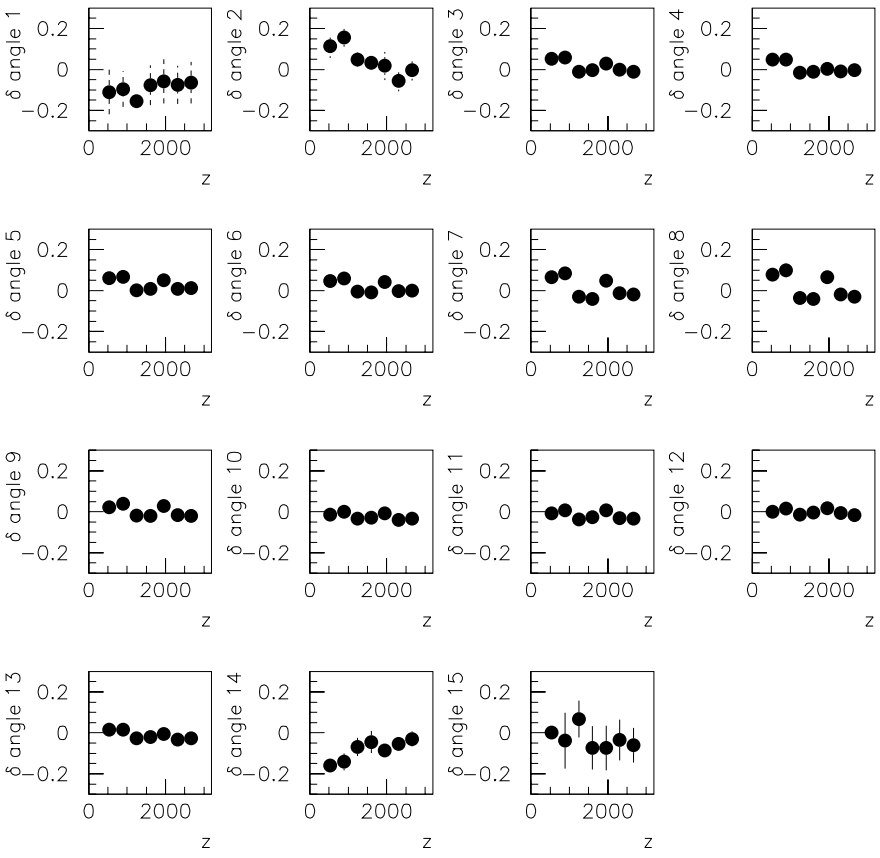

Figure 32: Difference in degrees, as a function of z, for all the angles of the absorber, between the measurement on both sides of the absorber

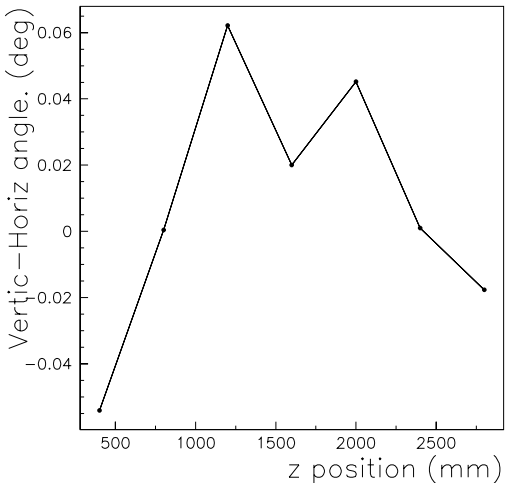

Figure 33: Average difference over the angles between horizontal and vertical angle measurements

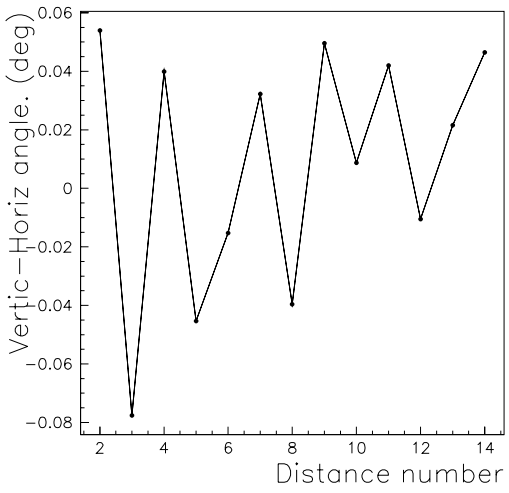

Figure 34: Average difference over the length of the absorber between horizontal and vertical angle measurements

5.3.2 Comparison between horizontal and vertical measurements

We have also compared the angle values, for the same absorbers measured in horizontal and vertical position. Figure 33 and 34 represent respectively the average of the difference over all the angles and over the z coordinate of the absorber. One notices that under its own weight, the absorber straight sections show a tendency to rotate around the bending lines, which causes the angle difference to alternate between positive and negative values: the opening of one fold causes the two adjacent ones to close, and vice-versa. All in all, it appears that the angles change by only very small amounts when going from horizontal to vertical position.

5.4 Distances between folds

The 11 distances between folds (see Fig 35) are measured by the CMM as described in section 4.1.

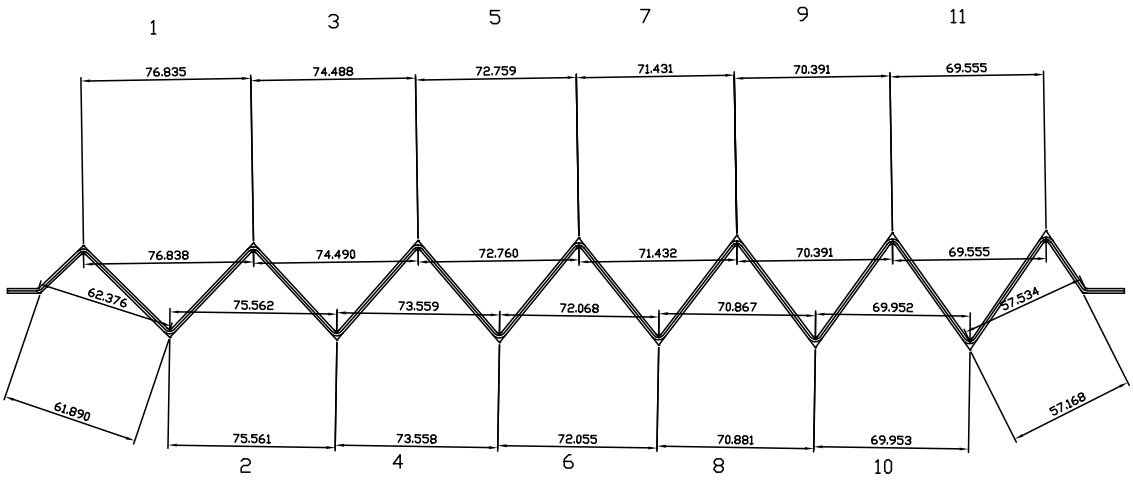

Figure 35: Theoretical values (in millimeters) of the distances between folds, as taken from the official drawing at 20 °C (ATLABEA_001)

The reproducibility of the measurements of the distances between folds is typically of the order of 30 μm (see Fig 36). Since the intrinsic reproducibility of the measurement is (see section 4.2) of the order of a few microns, this clearly hints towards variations during the production of the module 0 absorbers. Figure 37 shows the evolution of the fold distances as a function of the absorber number. These plots clearly show that the distance between folds have drifted over the construction of module 0. This is not very surprising, given the fact that the angles and the straight section lengths both have also drifted during the construction of module 0.

A study of the behaviour of the distance between folds along the absorber length shows that they are uniform to within 0.1 mm along the whole length of the absorber, the general tendancy being that they are smaller towards the middle of the absorber (see figures 38 and 39).

5.4.1 Comparison between horizontal and vertical measurements

As for the angles and the global dimensions, we have done comparisons between horizontal and vertical measurements, for the side accessible when the absorber was measured in horizontal position (cf Fig 40 and Fig 41). We observe as expected the same kind of behaviour on all these three kind of measurements, i.e. a global lengthening of the absorber when put into vertical dimension. The lengthening effect is not constant over z, but is most pronounced at the $z = 0$ and $z = 3200$.

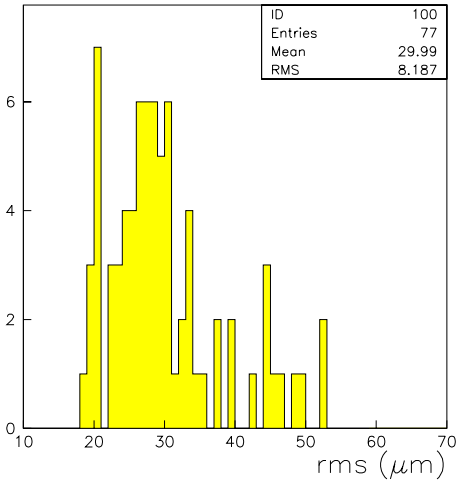

Figure 36: Distribution of the rms of all the distances between consecutive folds, using vertical measurements done from side A of the absorbeurs. Each entry is an rms among the 64 absorbers of Module 0

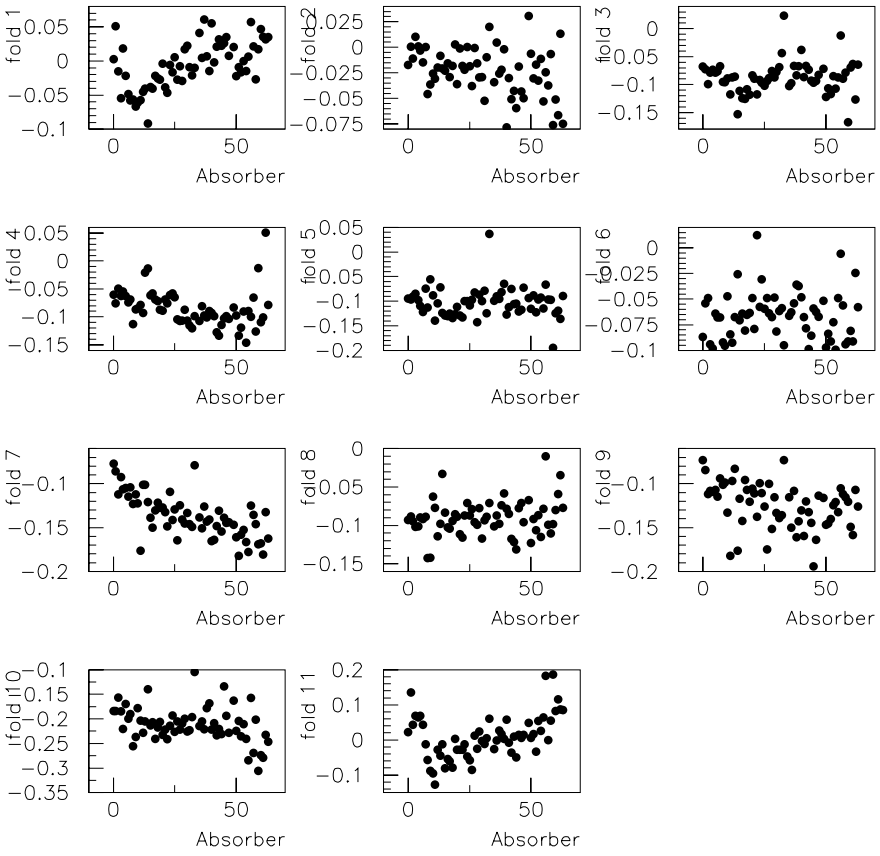

Figure 37: Evolution of the distances between folds as a function of absorber number, for module 0, at $z = 1200$. Theoretical values have been subtracted. Each plot represents one distance, and their numbering is the same as in figure 35

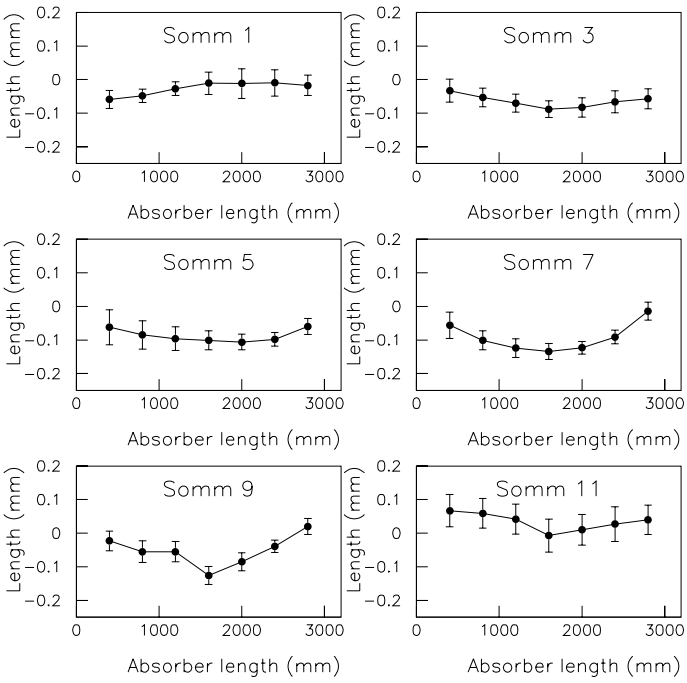

Figure 38: Variation of the distance between folds along the absorber length, for the angles open on side A. Data are taken from vertical measurements done from side A of the absorbers. The theoretical value is substracted for each entry

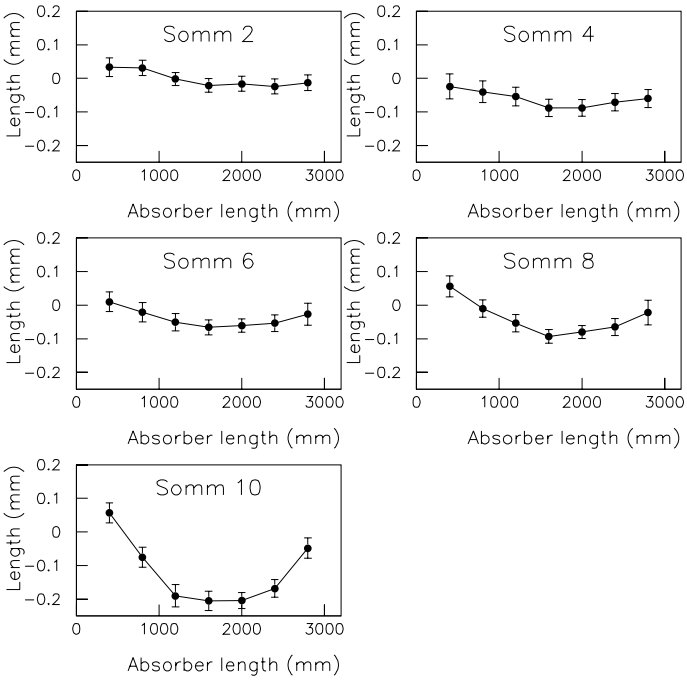

Figure 39: Variation of the distance between folds along the absorber length, for the angles open on side B. Data are taken from vertical measurements done from side A of the absorbers. The theoretical value is substracted for each entry

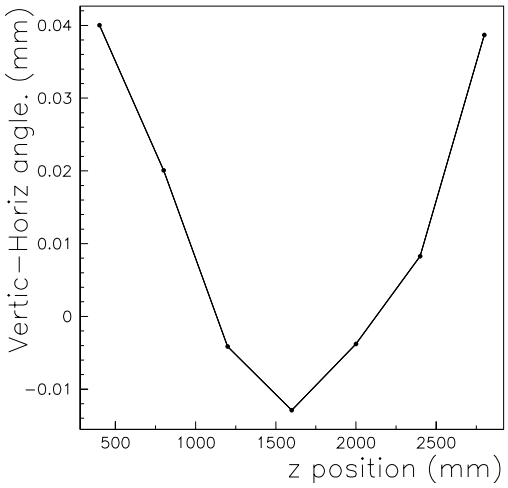

Figure 40: Average over the length numbers of the difference between horizontal and vertical measurements of the distance between folds

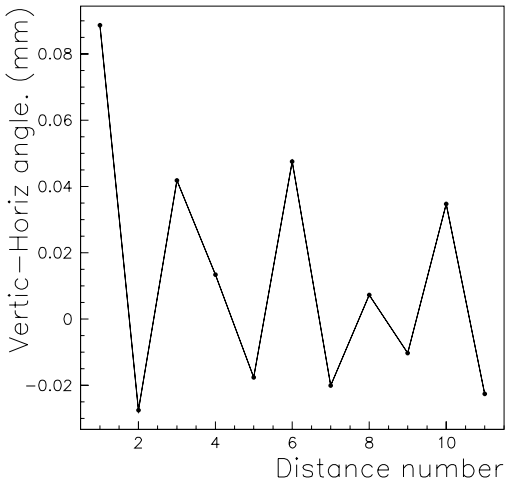

Figure 41: Average over the z coordinate of the absorber of the difference between horizontal and vertical measurements of the distance between folds

5.5 Thicknesses

Thicknesses are measured as described in section 4.1, using the vertical measurements only. The theoretical value of any of these measurement is 2.19 mm, on the whole absorber. The means of the straight section thicknesses, averaged over the 64 absorbers of Module 0, are given in Table 3 for all the measurement lines along the absorber length.

Straight Section	1	2	3	4	5	6	7	8	9	10	11	12	13	14
z(mm)														
400	.02	.01	.02	.02	.02	.02	.01	.03	.02	.02	.02	.03	.02	.01
800	.03	.03	.03	.04	.03	.04	.03	.05	.03	.03	.03	.04	.03	.02
1200	.01	.03	.02	.03	.02	.04	.01	.03	.02	.03	.02	.04	.02	.01
1600	.02	.01	.00	.02	.00	.02	.00	.02	-.01	.01	.00	.02	.00	-.01
2000	.01	.01	.00	.01	.00	.02	.00	.02	.00	.01	.01	.02	.01	-.01
2400	-.02	.00	-.01	.01	.00	.01	-.01	.01	.00	.01	.01	.02	.01	-.03
2800	-.02	-.01	-.02	.00	-.01	.00	-.01	.00	-.01	.00	.00	.01	.00	-.03

Table 3: Mean thickness (in millimeters) for the 64 absorbers of Module 0. The theoretical value (2.19 mm) is substracted for each entry

One can notice that the absorbers are too thick by typically 20 to 30 μm on the low-z, and almost at the theoretical value on the high-z side. The distribution of all the thickness measurements is given in Fig 43. On average, the thickness is 12 μm too high with respect to the theoretical value, with a dispersion of 32 μm. Figure 42 represents the distribution of the rms of all the measurements given in Table 3. Each entry is the rms among the 64 absorbers of a measurement at a given location in z and on a given straight section.

The reproducibility of the thickness measurements among the 64 absorbers of any of the thicknesses given in Table 3 is typically 30 μm or 1.4%. This is significantly higher than the intrinsic reproducibility of the measurement, that we conservatively have estimated in section 4.2 to be 10 μm. Plotting the average thickness of the absorbers as a function of absorber number gives us figure 44. Obviously, there are thickness variations along the whole production. These variations follow a slow trend associated with rapid fluctuations from absorber to absorber. The variations are even more striking if one plots one specific thickness measurement as a function of absorber number, as in figure 45 and figure 46. The changes in thickness observed on figure 45 and 44 around absorbers 45, 33 and 10 are neither related to a change of prepreg roll,

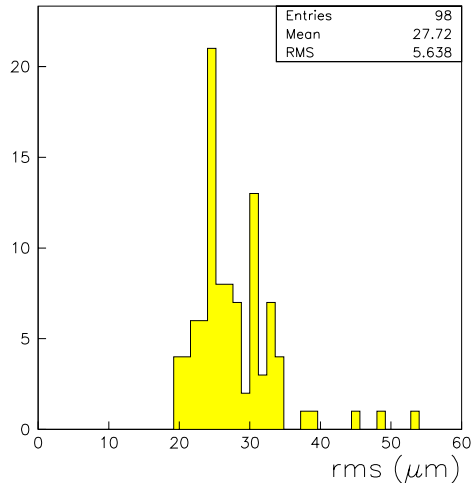

Figure 42: Distribution of the rms of all the thickness measurements. Each entry is the rms among the 64 absorbers of Module 0 of a variable whoose average value is given in Table 3

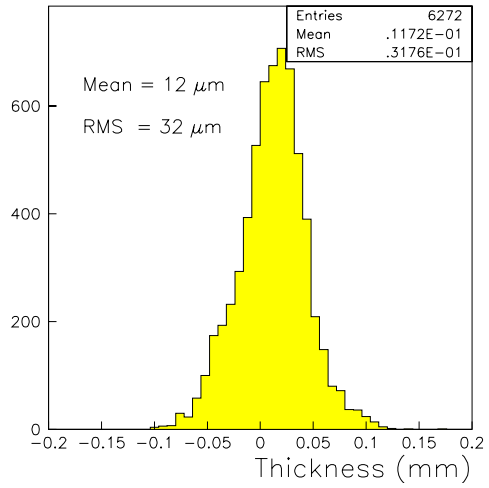

Figure 43: Distribution of the thicknesses for all measurements in z for all straight sections. The theoretical value is substracted for each entry

nor to the lead thickness. They were not understood at the time of M0 fabrication. Later on, these sudden changes in thickness were attributed to a thickness change in the prepreg rolls, even if the quality control reports of that material showed a constant thickness. No effect was observed on the thickness for any change in the bending machine tuning. The shape and the thickness are given by the gluing machine. We have also studied the thickness variations within one absorber. Figure 47 gives for example the average thickness of each measured line, as a function of z, for a few consecutive absorbers. As one can see, many shapes exist, with random changes from one absorber to its neighbours.

We can define an "average absorber" for the whole module 0 by taking, measurement point by measurement point on the absorber, the average of the 64 measurements done during the whole production of module 0. The thickness profiles of this average absorber are shown on figure 48 and 49. One can see that apart from the closest point to the side $\eta = 0$, there is a small constant decrease of the absorber thickness along the absorber length of 20 μm/m. On average, there is no tendancy for the thickness to follow a specific trend, as a function of straight section number. It is however interesting to note on figure 49 that the thickness depends on the parity of the straight section being measured. This can be interpreted as being due to a slight global translation of the upper mould of the gluing press : if the upper mould is translated in the plane of the absorber, so that the folding lines are slightly displaced with respect to the geometry given to the sandwich by the bending press, the net effect will be that every second straight section will tend to be thinner than average, and every other second will be slightly thicker. This effect is however very tiny.

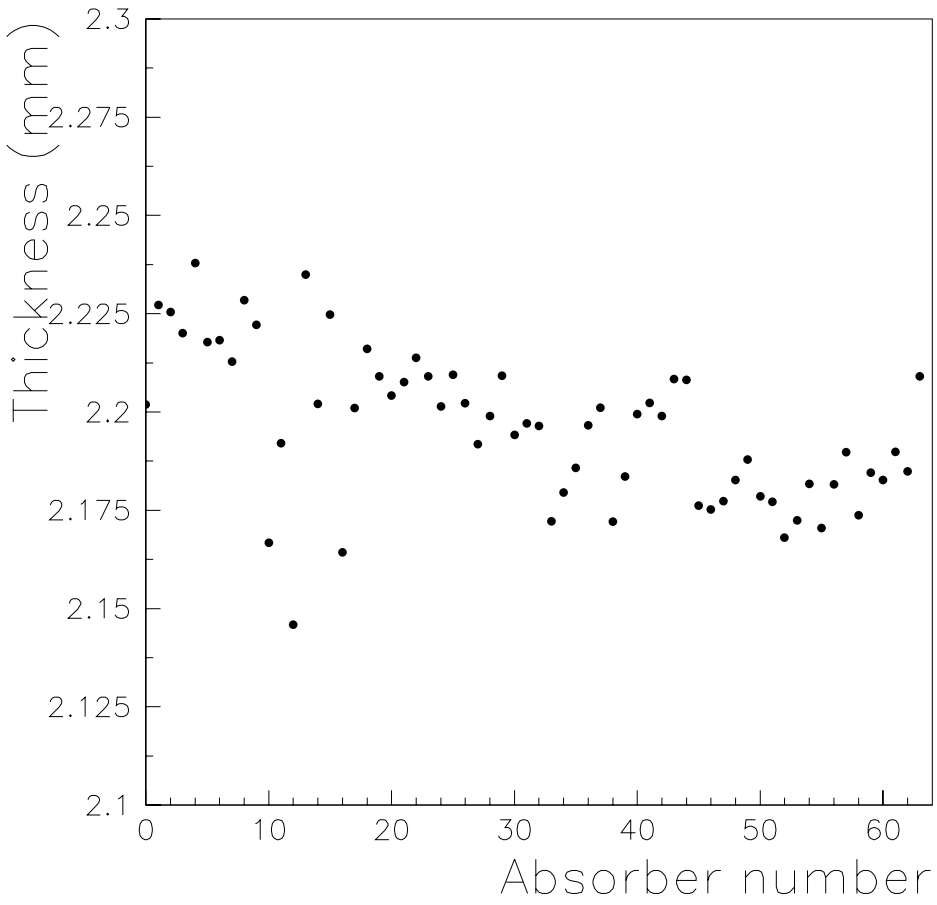

Figure 44: Average thickness of all absorbers as a function of absorber number

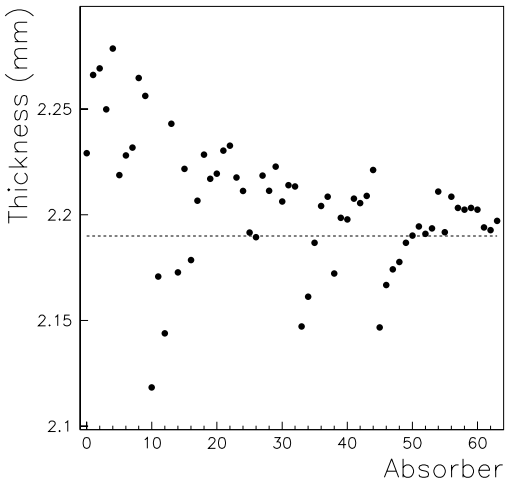

Figure 45: Thickness of straight section 7 at z=1200 mm as function of the absorber number. The dashed line corresponds to the theoretical value

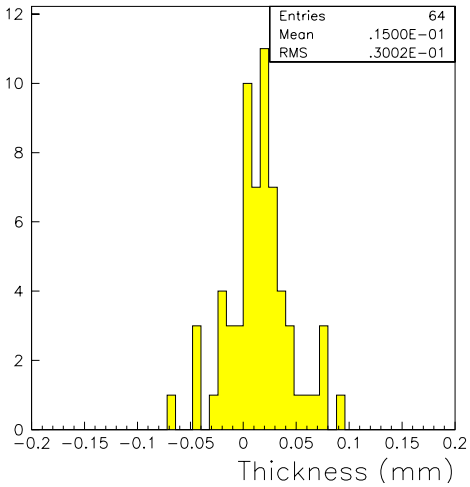

Figure 46: Distribution of the thicknesses of straight section 7 at z=1200 mm. The theoretical value is substracted for each entry

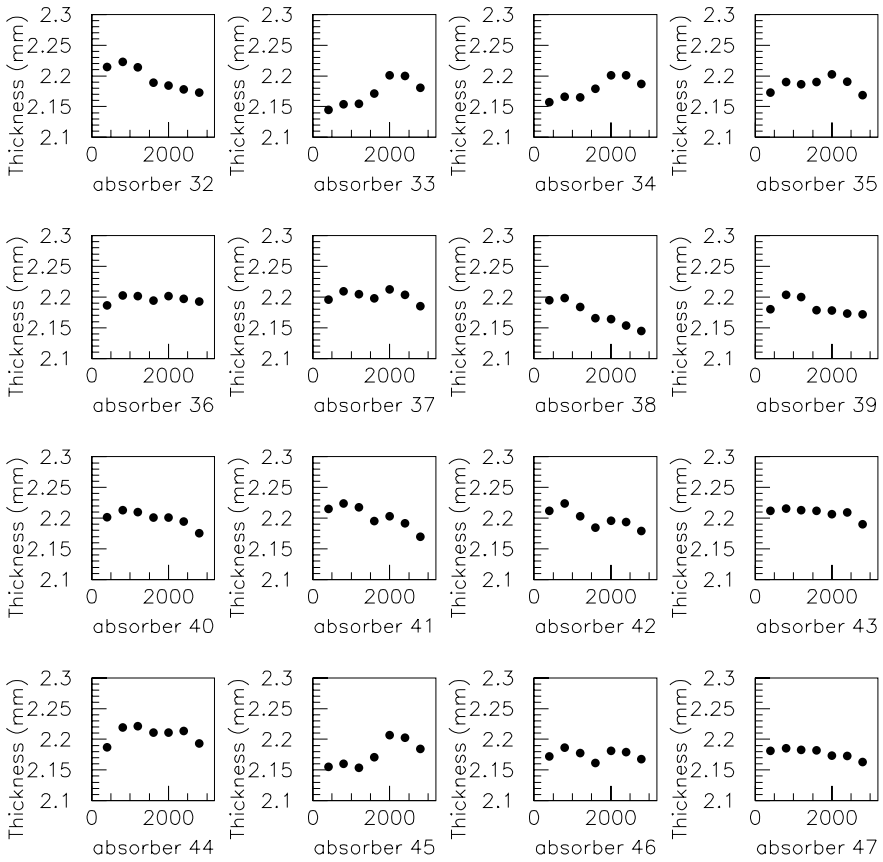

Figure 47: Thickness profiles of a few absorbers, as a function of z. The thickness of each measurement line is the average of all the thickness measurements on this line (one per straight section)

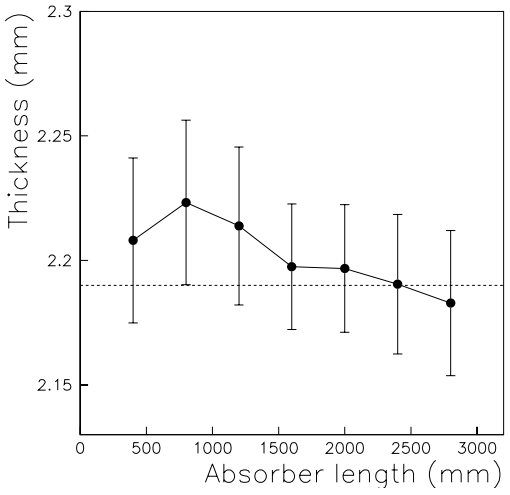

Figure 48: Variation of the thicknesses along the absorber length, integrated over straight sections # 1 to 14. The dashed line corresponds to the theoretical value

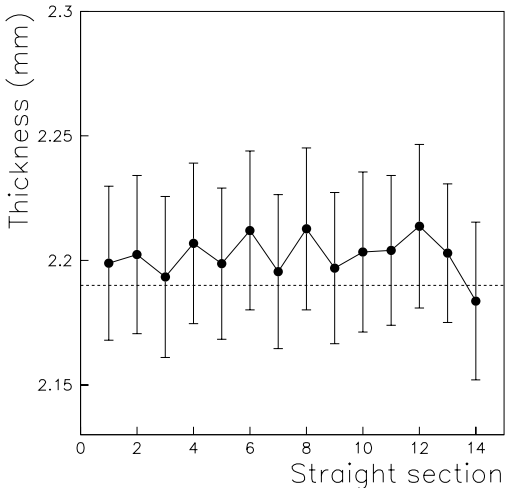

Figure 49: Variation of the thicknesses integrated over the absorber length. The dashed line corresponds to the theoretical value

5.5.1 Influence of lead thickness

The correlation between the ultrasonic lead thickness measurements and the output of the 3D machine [2] has been studied. This is shown on Fig 50, where the mean absorber thickness is plotted versus the mean of the ultrasonic measurements for absorber #13 to 63. No correlation is observed, which implies that the variations of the absorber thicknesses are not due to the lead itself, but to the prepreg and gluing process.

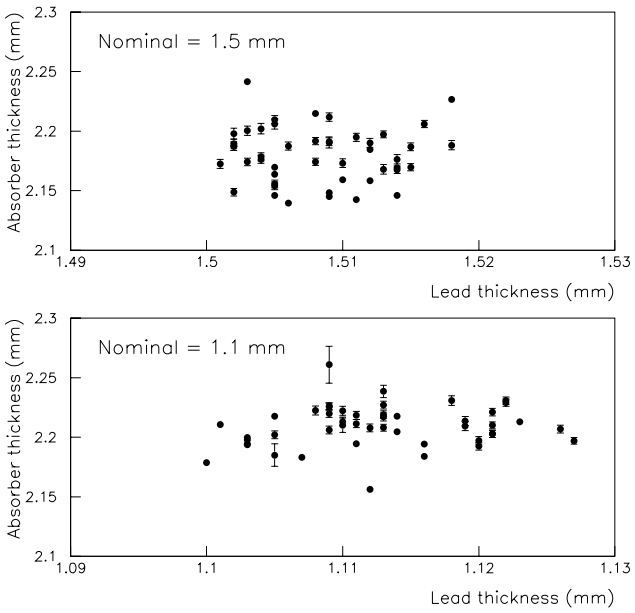

Figure 50: Correlation between lead and absorber thicknesses for both nominal lead thicknesses

5.6 Global shape

Although the folding lines of the absorber are not rigorously coplanar, they are very close to (cf Fig 51). The deviation from the coplanarity is of the order of a few microns. This allows us to define the opening angle of the absorber as the angle between the two planes containing the folding lines. Figure 52 gives the distribution of this global shape estimator. As can be seen, the opening angle is slightly smaller than expected.

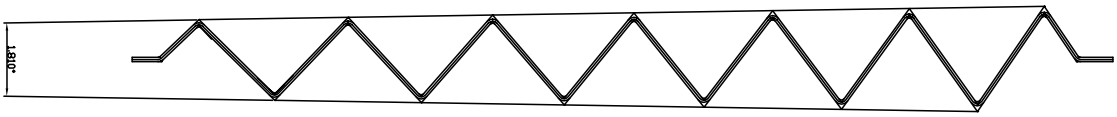

Figure 51: Definition of the opening angle of the absorber

We have also investigated the tridimensional shape of the absorber. To do that, we have reconstructed the position of the intersections between the straight sections and the central plane of the absorber. Figure 53 gives the information we used to reconstruct these positions : we use the knowledge between the distance of the straight section extremities (which we know from the measurements) and the point we are looking for. Of course, this relies on the hypothesis that the displacements we are trying to measure are larger than the typical length variations of the straight sections.

Figure 54 shows for a few absorbers the tridimensional maps of the positions of the coplanar points we have defined, as a function of the z position along the absorber (positive coordinate on figure 54) and as a function of the r coordinate of the absorber (negative coordinate on figure 54). If the absorbers were flat, all the points computed using the information of figure 53 would be coplanar and all the plots of figure 54

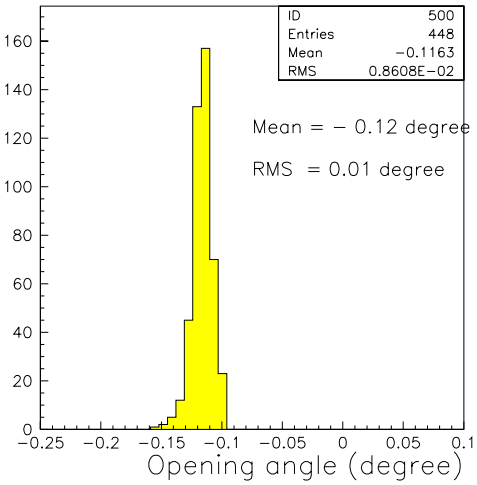

Figure 52: Mean opening angle of the absorbers, as defined in text. The theoretical value is substracted for each entry

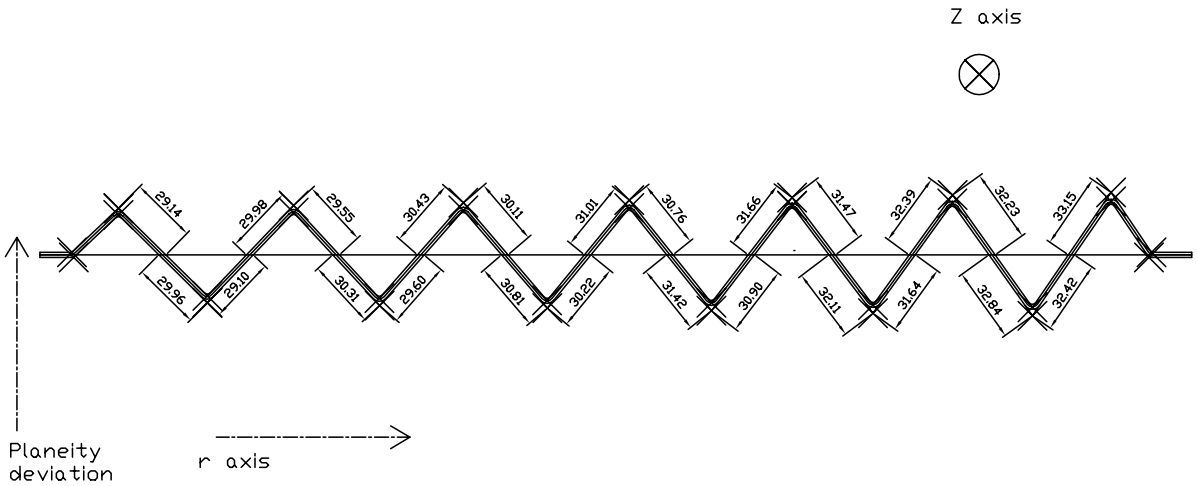

Figure 53: Positions of the coplanar points used to study the global shape of the absorber

would be planes. As can be seen from figure 54, the deviation from flatness is typically of the order of 1 mm, and the shape of the absorber is close to an helix.

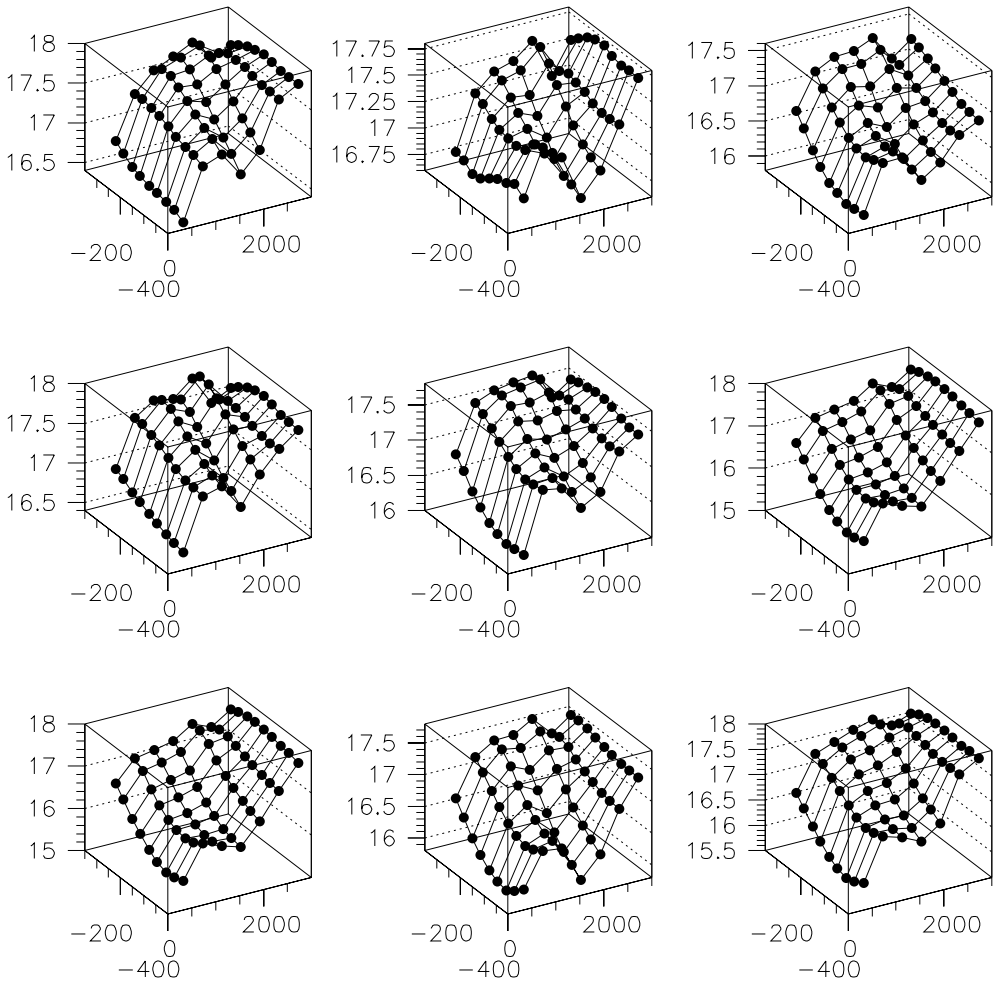

Figure 54: Actual tridimensional maps of the absorber planes, for 9 different absorbers. The positive coordinate is z, the negative is r. The vertical coordinate is the offset of the coplanar points of figure 53 with respect to the (r,z) plane

6 Conclusion

In this work, we have first evaluated the performance of the tridimensional coordinate measuring machine used to control the barrel absorbers. The performance of the measurements is summarized in the following table :

Meas. quantity	Typical value	Measurement accuracy
Straight section length	60 mm	4 μm
Global dimensions, widths	160 mm to 540 mm	160 mm : 0.12 mm 540 mm : 0.16 mm
Angles	90°	0.004°
Thickness	2.19	0.01 mm (conservative)

Table 4: Performance of the measurement process

The deviations we have observed from the theoretical dimensions can be summarized in the following table :

Meas. quantity	Avg. deviation	r.m.s.	Comments
Straight section length	+60 μm (central sections) +200 μm extremities	20 μm 20 μm	Slow drifts observed Slow drifts observed
Global dimensions, widths	+100 μm to +400 μm	150 μm	Slow drifts Strong z dependance
Angles	$-0.2°$	$0.15 - 0.50°$	Slow drifts, section dependant
Thicknesses	0-30 μm		Drifts and sudden changes observed

Table 5: Deviation from theoretical value of the average absorber

As can be seen in Table 5, the deviations between the experimental geometrical quantities and their theoretical values are all very small. For the series, it is planned to measure all the absorbers to have a complete record of the absorber production. However, it should be noticed that for the series, it will not be possible in general to measure the absorbers immediately after bending, due to a delay in the G10 bars delivery, that has forced the collaboration to store the bent absorbers without bars glued to them. This will of course reduce the possibility of reaction in case of a problem. However, the production of module 0 has proven that the tooling used is quite stable, so this should not be a problem.

7 Acknowledgements

We would like to thank B. Mansoulié for fruitful advices and discussions. We also would like to thank J.M. Noppe and D. Imbault, and all the staff of our laboratories involved in the fabrication and measurements of all the module 0 absorbers.

References

[1] Liquid Argon Technical Design Report, pp 172-178

[2] ATL-LARG-98-107. The offline lead thickness measurement system for the ATLAS Electromagnetic Calorimeter, P. Beauchet et al.